

# Unified QCD picture of hard diffraction

H. Navelet and R. Peschanski  
 Service Physique Theorique, CE Saclay\*†

December 24, 2018

## Abstract

Using a combination of S-Matrix and perturbative QCD properties in the small  $x_{Bj}$  regime, we propose a formulation of hard diffraction unifying the partonic (Ingelman-Schlein) Pomeron, Soft Colour Interaction and QCD dipole descriptions. In particular, we show that all three approaches give an unique and mutually compatible formula for the proton diffractive structure functions  $F_{T,L}^{Diff}$  incorporating perturbative and non perturbative QCD features.

## 1 Introduction

“Hard diffraction” is an experimental phenomenon which lies at the borderline between “hard” and “soft” interactions. It appears as a scattering process initiated by a hard probe (e.g. a virtual photon at HERA [1] or a forward jet at the Tevatron [2]), but in which the proton target is not destroyed, in a similar way to conventional soft diffractive processes. It is associated with large rapidity gaps between the hadronic remnants of the target and of the projectile as was discovered at HERA, but was first identified by high- $P_T$  jets in diffraction at the ISR [3].

There has been a lot of debate about the theoretical explanation of hard diffraction. Indeed, assuming a partonic content of the Pomeron led to a

---

\*Address: SPhT CEA-Saclay F-91191 Gif-sur-Yvette Cedex, France;

†emails: navelet@sph.t.saclay.cea.fr, pesch@sph.t.saclay.cea.fr

nice prediction [4] of the phenomenon and, supplemented by the QCD evolution of diffractive structure functions, to a quantitative description of HERA data [5]. As satisfactory as can be this phenomenological analysis, the main unsolved problem in this approach is the lack of relation between diffractive and non diffractive hard scattering leading to a profusion of input parameters (e.g. the non-perturbative parton distributions in the Pomeron). If one wants to enter more deeply in the study of hard diffraction and in the still mysterious nature of the Pomeron interaction, one has to look for theoretical links with QCD. This is our goal.

In the present paper, we shall focus on three existing different theoretical approaches of hard diffraction, for which we propose a new, unifying, formulation. The first one we will refer to is the “partonic Pomeron” approach [4]. The hard photon is here supposed to probe the parton distributions of the Pomeron Regge pole considered as a hadronic particle. In fact we can also consider it as an extension of the Regge theory of soft diffraction [6] to incorporate the effect of the hardness of the probe<sup>1</sup>.

A second approach is the Soft Colour Interaction one, where hard diffraction is described by a two-step process: during a relatively short “interaction time”, the probe initiates a typical hard deep-inelastic interaction. Then, at large times/distances, a soft colour interaction is assumed which will decide of the separation between diffractive and non-diffractive events according to a simple probabilistic rule: It gives rise to colour neutralization of the final state with probability of order  $1/N_c^2$  (where  $N_c$  is the number of colours) and thus to rapidity gaps and diffraction. The assumed extreme softness of Soft Colour Interaction ensures that the dynamics of hard partons remains unchanged. Various models based on Soft Colour Interaction [8, 9] lead to satisfactory phenomenological descriptions.

A third approach is based on the small  $x_{Bj}$  regime of perturbative QCD, where the resummation of leading  $\log 1/x_{Bj}$  contributions allows one to obtain some theoretical information on high energy hard interaction processes following the Balitsky, Fadin, Kuraev, Lipatov (BFKL) approach [10]. Calculations of hard diffraction using the related QCD dipole approach [11] or in the original BFKL framework [12] have been performed. In fact, in the line of QCD dipole models for proton structure functions [13], models [14]

---

<sup>1</sup>Models using explicitly concepts of the S-Matrix framework of Regge singularity theory and taking into account the hard probe on a phenomenological ground do exist [7].

for diffractive proton structure functions<sup>2</sup> have been derived and give a convenient description of HERA data. For further abbreviation we shall call it the “QCD dipole” approach<sup>3</sup>.

Keeping a general point of view, one may notice that each of these approaches has advantages and disadvantages with respect to the others. The partonic Pomeron approach synthesises what we know about the effect of the hard probe and the factorization properties of the hard interaction but gives no prediction about the soft Pomeron dynamics. The Soft Colour Interaction approach give a nice relation (even in normalization) between hard and soft deep-inelastic scattering but the nature of the colour rearrangement at long distances is unknown. Finally the QCD dipole approach gives detailed prescriptions for the form of the amplitudes, but the problem of the perturbative/non-perturbative QCD interface and the crucial point of the relative normalization of diffractive *vs* non-diffractive contributions, remain obscure.

In the present paper we will show that the three approaches may find a common formulation and intrinsic mutual equivalence through S-Matrix relations on different analytic discontinuities of  $3 \rightarrow 3$  forward elastic amplitudes in the so-called triple-Regge regime. Within this unifying S-Matrix framework and using the hard probe as a hint for the application of perturbative QCD to the calculation of these discontinuities whenever it is reasonably justified, we will end with a constrained formulation of the diffractive structure functions, transcending the limitations of each of them taken separately.

The plan of the paper is as follows: In the next section we will give the general framework, using both the S-Matrix and perturbative QCD properties, allowing one to mutually relate the three abovementioned approaches to hard diffraction. In the next section 3, concentrating on the *inelastic* component, we show the compatibility of the QCD dipole and partonic Pomeron approaches. In section 4 the same is done for the QCD dipole and Soft Colour Interaction approaches. As a result, a determination of the longitudinal and transverse diffractive structure functions emerges incorporating both perturbative and non perturbative ingredients in an overall consistent QCD picture of hard diffraction. In the last section 5, we give a summary of our results, and an outlook on phenomenological tests and theoretical consequences of

---

<sup>2</sup>Two different components have to be distinguished [15, 14] : *inelastic* for large diffractive masses and *elastic* for small masses.

<sup>3</sup>To be more specific, we shall not include either next-leading or non-perturbative corrections to the QCD dipole picture, and use an effective leading order BFKL approach.

our unifying approach.

## 2 General unifying framework

The usual kinematical variables for the diffractive amplitudes and cross-sections are  $Q^2$ , the photon virtuality,  $Y \equiv \log 1/x_{Bj}$ , the total rapidity available for the final hadronic state,  $y \equiv \log 1/x_P$ , the rapidity gap,  $t \simeq -P_T^2$ , where  $P_T$  is the momentum transferred at the proton vertex. We use also  $Y-y \approx \log M_X^2 \simeq \log 1/\beta$  where  $M_X$  is the invariant mass of the diffractively produced state<sup>4</sup>.

In the following we shall make use of the important S-Matrix connection, also called Mueller-Regge relation [17], between semi-inclusive amplitudes and specific discontinuity contributions of forward elastic  $3 \rightarrow 3$  amplitudes. It naturally applies to hard diffraction initiated by a virtual photon, as sketched in Fig.1, namely

$$\gamma^* + p \rightarrow p + X \iff \text{Disc}_1 \{ \gamma^* \bar{p} \, p \rightarrow \gamma^* \bar{p} \, p \} . \quad (1)$$

In fact, this relation, derived in the context of soft physics<sup>5</sup> [18], can also be applied to the definition of hard diffraction when  $Q^2$  and  $y \equiv \log 1/x_P$  are large enough (typically,  $Q^2 > 4.5 \text{GeV}^2, x_P > 10^{-2}$ ). In this case, the Mueller-Regge relation applies in a region where the Pomeron Regge poles are supposed to take into account the colour singlet exchange responsible for the gap. If moreover, the diffractive mass  $M_X$  is large enough, one considers a Pomeron-like singularity describing the large  $M_X$  behaviour. However the resulting triple-Pomeron contribution is to be interpreted here in a loose sense since this third Regge singularity may differ from the other ones due to the hard probe, as mentionned in the previous section. We will thus keep the word Pomeron for those responsible for the gaps.

In the triple-Regge kinematical region, one thus writes [6]:

$$\frac{dF_{T,L}^{\text{Diff}}}{dP_T^2} \sim \text{Disc}_1 A(3 \rightarrow 3) \propto G_P(t) |\xi_{\alpha_P}|^2 e^{2(\alpha_P-1)y} \sigma_{\gamma^* - P}^{\text{tot}} , \quad (2)$$

---

<sup>4</sup>Indeed one has the relation  $\beta \equiv x_{Bj}/x_P = Q^2/(M_X^2 + Q^2 - t)$  but due to the sharp cut-off in  $t$ , one can often neglect  $t$  in the denominator.

<sup>5</sup>To our knowledge, the application of the Mueller-Regge relations for the Soft Pomeron region appeared in a Regge theory framework in Refs.[18], while the phase factors were discussed in detail in [19]. The extension to soft diffraction and related references can be found in Ref. [6].

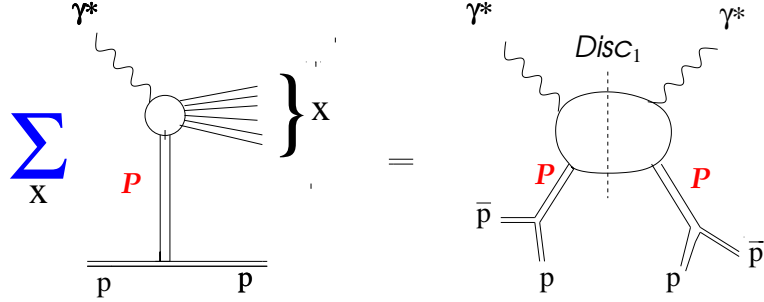


Fig. 1

Figure 1: **Mueller-Regge relation for hard diffraction.** The summation over final diffractive states  $\mathbf{X}$  gives rise to a specific discontinuity  $Disc_1A$  of a forward  $A(3 \rightarrow 3)$  amplitude.  $P$  denote the Pomeron-Regge exchange leading to rapidity gaps .

where  $\frac{dF_{T,L}^{Dif}}{dP_T^2}$  is the “unintegrated” ( $t$ -dependent) diffractive structure functions (related to the measurable hard diffractive cross-sections),

$$\xi_{\alpha_P}(t) \equiv \Gamma(-\alpha_P(t)) \left\{ 1 + e^{-i\pi\alpha_P(t)} \right\} \quad (3)$$

is the (partonic) Pomeron Regge phase factor in the amplitude and  $\alpha_P(t) = \alpha_P(0) + \alpha'_P t$  is the (partonic) Pomeron-pole Regge trajectory<sup>6</sup> with intercept  $\alpha_P(0)$  and slope  $\alpha'_P$ .  $G_P(t)$  is a function, not constrained in the Regge formalism, describing the coupling of incident Pomerons to the proton.

The Pomeron-photon cross-section  $\sigma_{\gamma^* - P}^{tot}$  describes the interaction of the hard probe with the incident Pomeron. For instance, in the partonic Pomeron model [4] , it is expressed in terms of Pomeron structure functions, in much the same way as proton-photon cross-sections are expressed in terms of the proton structure functions, but with a quite different partonic content [5].

Quite interestingly, the existence of the Regge phase factors (3) allows one to relate other discontinuities of  $A(3 \rightarrow 3)$  to  $Disc_1A$ . As sketched in Fig.2, one may consider a double discontinuity  $Disc_2A(3 \rightarrow 3)$  taking into account also the analytic discontinuity in the subenergy of one of the incident Pomeron exchanges and then a triple discontinuity  $Disc_3A(3 \rightarrow 3)$  including

<sup>6</sup>Other Regge singularities, such as cuts, could appear and give logarithmic prefactors. For sake of simplicity, but without affecting the conclusions, we will stick to the formalism of “effective” Regge poles.

the discontinuity over the two Pomeron exchanges. The expression of the discontinuities, through generalized unitarity relations, is obtained through the imaginary part of the relevant Regge phase factors. One writes<sup>7</sup> [19]:

$$Disc_1 A = Disc_2 A = Disc_3 A = \frac{\sin \pi(2\alpha_P(t) - \alpha_P^*(0))}{\sin \pi\alpha_P^*(0)} \mathcal{V}_{p\bar{p}}, \quad (4)$$

where  $\mathcal{V}_{p\bar{p}}$  is a real function describing the  $p\bar{p}$  vertex in  $A(3 \rightarrow 3)$ . The notation  $\alpha_P^*(0)$  indicates that the third Regge exchange, corresponding to the summation over diffractive final states, may have (and indeed *has* in our calculations) a different effective trajectory<sup>8</sup>.

Beyond these general relations of the S-Matrix framework in the triple-Regge regime, we will now take advantage of the hard probe, allowing one to introduce in the game the (resummed) perturbative QCD expansion at high energy (small  $x_{Bj}$ ).

Let us start with general considerations. In a generic S-Matrix approach, the analytic discontinuities of scattering amplitudes are related to a summation over a complete set of asymptotic *hadronic* final states. If however, the underlying microscopic field theory is at work with small renormalized coupling constant due to the hard probe, it is possible in some cases to approximate the same discontinuity using a complete set of *partonic* states. In particular, at high energy and within the approximation of leading logs (and also large  $N_c$ ), QCD dipoles can be identified as providing such a basis [11]. The interest is that the wave function of incoming states at the hard vertex is completely determined at the leading log level. Using this wave-function<sup>9</sup> together with the appropriate  $k_T$  factorization properties at the proton vertices [20], one is able to estimate the contributions to the various discontinuities of  $A(3 \rightarrow 3)$  depicted in Fig.2 within the (resummed) perturbative QCD framework.

Hence, the S-Matrix relations (4), which express a simple phase relation in a pure Regge framework, acquire a non-trivial meaning if one considers the various perturbative QCD ingredients and non-perturbative interfaces for the

---

<sup>7</sup>The derivation can be found in the Physics Reports of Ref. [19] with the complete expressions in page 319 for the cut and uncut triple-Regge vertices. The main issue is that the single discontinuity  $Disc_1$  eliminates already all terms but one in the rather involved expression of the uncut vertex.

<sup>8</sup>In particular,  $\alpha_P^*(0) \neq 1$ , avoiding a definition problem in (4).

<sup>9</sup>In fact only  $1 \rightarrow 1$  and  $1 \rightarrow 2$  dipole transitions are needed [11, 14].

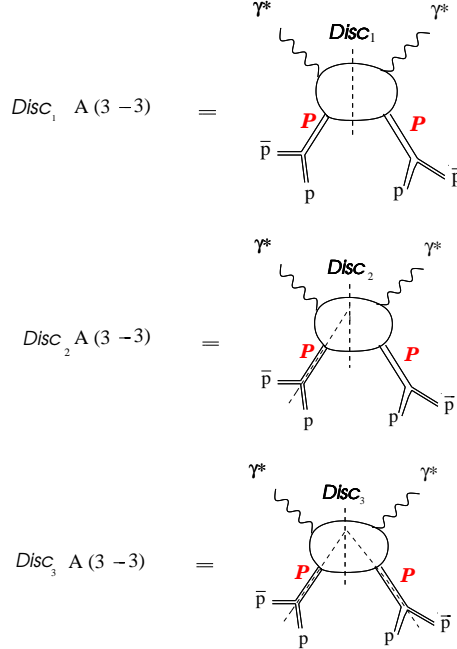


Fig. 2

Figure 2: **Three analytic discontinuities of  $A(3 \rightarrow 3)$ .** The single  $Disc_1 A$ , double  $Disc_2 A$ , and triple  $Disc_3 A$  discontinuities of the triple-Regge  $A(3 \rightarrow 3)$  amplitude are displayed .

different discontinuities. In some sense, as it is shown in Fig.3, the discontinuities can be associated, whenever it is possible, with the hard QCD interaction at some time  $T \approx 1/Q$ , supplemented by a perturbative resummation of QCD radiation around this interaction time. The perturbative/non-perturbative interface has to be taken into account in order to put a reasonable limit to this derivation. Depending on the discontinuity considered, one has different interaction pictures with a hard interaction at short time, and soft interaction diluted in space-time. Instead of considering these pictures as different, we will use the S-Matrix relations as a link between these pictures and thus will get non-trivial relations, as we will see later on. Let us comment in turn on the pictures corresponding to  $Disc_1$ ,  $Disc_2$ ,  $Disc_3$ .

**i)**  $Disc_1$ , as we have seen from relation (2), is parametrized in terms of soft Pomeron trajectories and of  $\sigma_{\gamma^* - P}^{tot}$ , the unknown quantity parametrizing the

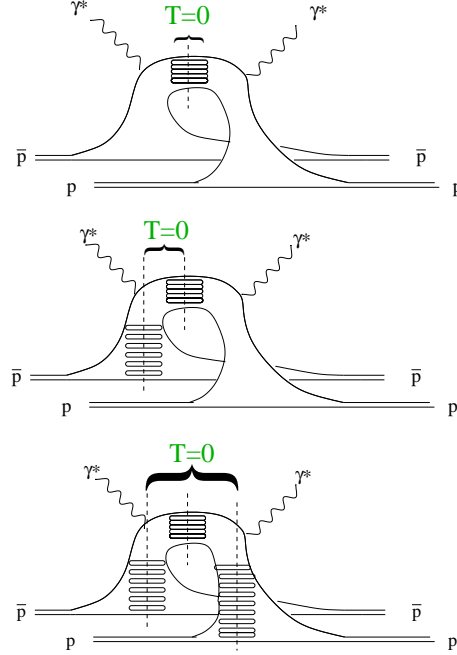


Fig. 3

Figure 3: “Time-dependent” picture of the  $A(3 \rightarrow 3)$  discontinuities. Upper graph: Description of  $Disc_1 A(3 \rightarrow 3)$  (partonic Pomeron approach); Middle graph: Description of  $Disc_2 A(3 \rightarrow 3)$  (candidate for the Soft Colour Interaction approach); Lower graph: Description of  $Disc_3 A(3 \rightarrow 3)$  (QCD dipole approach).

interaction of the incident Pomeron with the hard probe. The same  $\sigma_{\gamma^* - P}^{tot}$  is the one described by the partonic structure functions of the Pomeron in the original scheme of Ref.[4].  $Disc_1$  is thus a natural framework for the partonic Pomeron approach, since the analytical discontinuity over the diffractive final states is effectively expressed in terms of the hard interaction of the photon with the partons inside the incident Pomeron. This is schematically depicted in the “time-dependent” scheme of Fig.3, where the soft incident Pomerons are represented as living during a “long” time, while the partonic (or QCD dipole) process is initiated by the hard interaction.

ii)  $Disc_2$  is quite interesting since it appears as a good candidate for a description of the Soft Colour Interaction approach, see Fig.3. It appears as a partonic interaction very similar to the one describing ordinary deep-

inelastic processes, in parallel with a “soft” correction evolving during a long time, corresponding to the uncut Pomeron singularity in Fig.3. In section 4, we will see how this can be quantified using the interrelation with the QCD dipole picture.

**iii)  $Disc_3$**  : In this case the discontinuity is the “full” one, cutting the two Pomerons together with the  $\gamma^* - P$  interaction. Indeed, this full cutting is required by consistency of the QCD dipole picture based on a QCD calculation of the partonic states at the interaction time [11]. In the description of hard diffraction (see, e.g., [11], the amplitude is deduced from a  $1 \rightarrow 2$  dipole transition, starting either from the primordial  $q\bar{q}$  state of the photon (“elastic component”) or from a dipole excited in the photon wave function for higher diffractive masses (“inelastic component”). In the following we shall focus on the main “inelastic component”, leaving the “elastic component” for a further study<sup>10</sup>.

This last analysis requires some more care about the perturbative/non-perturbative interface, which cannot be restricted to usual factorisation properties. As studied in Ref. [22], one has to distinguish the cases whether we consider strictly the forward  $t = 0$  case or not. Indeed, whenever  $t \neq 0$ , the QCD radiation accompanying the hard probe extends far into the infrared region at the triple Pomeron vertex, making the perturbative treatment difficult. At  $t = 0$ , due to an interesting conservation law of conformal dimensions in the BFKL framework, the perturbative resummation acquires more credibility, at least in the same approximation as for the total structure functions,. We will thus stick to using the perturbative calculations at  $t = 0$ , more precisely inspiring ourselves from those performed in paper Ref. [23] in the framework of the QCD dipole model<sup>11</sup>.

Due to the relations (4), we expect that all three descriptions of hard diffraction, even if having seemingly distinct “time evolutions”, indeed correspond to an unique one in a complete QCD theory satisfying both macroscopic (S-Matrix) and microscopic (with interacting quarks and gluons) requirements. In the absence yet of such a complete realization of the strong

---

<sup>10</sup>We expect the “elastic component” to be related to higher twist terms in an operator product expansion of diffractive structure functions [21].

<sup>11</sup>These calculations are similar to those performed in the BFKL framework [22], with the simplification that the 4-gluon intermediate state does not appear in the  $1/N_c$  limit of the QCD dipole model. The inclusion of such a state will be welcome, especially for large diffractive masses, but lies beyond the scope and the dipole framework of our present paper.

interaction theory, we shall adopt the following point of view: looking for a synthesis, we will first check whether all three approaches are consistent between themselves and then formulate hard diffractive structure functions realizing the synthesis.

### 3 From QCD dipoles to partonic Pomeron

Our starting point is the formula for the differential structure functions (inelastic component) at  $P_T=0$  for longitudinal and transverse photon given in [23]:

$$\begin{aligned} \frac{dF_{T,L}^{Diff}}{dP_T^2}(Q^2, Y, y; P_T=0) &= \\ &= \frac{\mathcal{N}^{Diff}}{x_P Q_0^2} \int_{c-i\infty}^{c+i\infty} \frac{d\gamma_1}{2i\pi} \frac{d\gamma_2}{2i\pi} \frac{d\gamma}{2i\pi} \delta(1-\gamma_1-\gamma_2-\gamma) \Theta P f_{T,L} \\ &\times \left(\frac{Q}{Q_0}\right)^{2\gamma} \exp\{y[\Delta(\gamma_1) + \Delta(\gamma_2)] + (Y-y)[\Delta(\gamma)]\} , \end{aligned} \quad (5)$$

where

$$\Delta(\gamma) \equiv \frac{\alpha_s N_c}{\pi} \chi(\gamma) = \frac{\alpha_s N_c}{\pi} \{2\psi(1) - 2\psi(\gamma) - 2\psi(1-\gamma)\} \quad (6)$$

is the BFKL evolution kernel [10],  $Q_0$  the non-perturbative scale of primordial dipoles in the proton [13],

$$\mathcal{N}^{Diff} \equiv \frac{2\alpha_s^5 N_c^2 e_f^2}{\pi^3} n_{eff}^2, \quad (7)$$

the normalization with  $n_{eff}$  the phenomenological number of primordial dipoles in the proton at scale  $Q_0$  and  $e_f^2$  the sum over squared quark charges. The other prefactors of perturbative QCD origin are:

$$P f_{T,L} \equiv h G(\gamma_1) h G(\gamma_2) I_{T,L}(\gamma) G^{-1}(\gamma) , \quad (8)$$

with

$$h(\gamma) = \frac{1}{4\gamma^2(1-\gamma)^2} ; \quad G(\gamma) = \frac{\Gamma(\gamma)}{\Gamma(1-\gamma)} , \quad (9)$$

and finally,

$$\begin{pmatrix} I_L \\ I_T \end{pmatrix} \equiv \frac{1}{\gamma(1-\gamma)} \frac{\Gamma^2(1+\gamma)\Gamma^4(2-\gamma)}{\Gamma(4-2\gamma)\Gamma(2+2\gamma)} \begin{pmatrix} 2\gamma(1-\gamma) \\ (1+\gamma)(2-\gamma) \end{pmatrix},$$

which are the ‘‘impact factors’’ [10, 20, 13] of the longitudinal and transverse photon in the BFKL formalism.  $\Theta$  is a cut-off function taking into account the non-perturbative description of the end of the rapidity spectrum of emitted gluons [23]. In practice, it mainly affects the overall normalization (also the form at edges of the  $\beta$ -dependence). It is one aspect of the lack of predictivity of the QCD dipole approach about the relative normalization of diffractive vs. non diffractive contributions.

One important ingredient of formula (5) is the delta function  $\delta(1-\gamma_1-\gamma_2-\gamma)$ . It expresses the conservation law of conformal dimensions at the triple pomeron vertex, which is a special feature of the BFKL property in the forward direction. As discussed in the previous section, we have chosen the QCD dipole formulation for the forward diffraction instead of the non-forward one [11], since it is expected to be less affected by non-perturbative contributions. On the other hand, it is phenomenologically not difficult to insert the non-perturbative phenomenological information on the  $t$ -dependence coming from the proton vertices in the non-forward region. Indeed, it is convenient to parametrize the integrated diffractive structure function assuming an exponential behaviour  $\frac{dF_{T,L}^{Diff}}{dP_T^2} \approx \frac{dF_{T,L}^{Diff}}{dP_T^2}(P_T = 0) e^{-P_T^2/\langle P_T^2 \rangle}$ , well verified experimentally<sup>12</sup> [24]. We will thus in the following assume the relations:

$$F_{T,L}^{Diff}(Q^2, Y, y) \equiv \int dP_T^2 \frac{dF_{T,L}^{Diff}}{dP_T^2} \approx \langle P_T^2 \rangle \frac{dF_{T,L}^{Diff}}{dP_T^2}(P_T = 0). \quad (10)$$

The first step of the computation of formula (5) is [12, 23] to use the saddle-point approximation at large  $y$  to integrate over the difference  $\gamma_1 - \gamma_2$ . One easily gets

$$\frac{dF_{T,L}^{Diff}}{dP_T^2}(P_T = 0) = \mathcal{N}^{Diff} \frac{1}{x_P Q_0^2} \int_{c-i\infty}^{c+i\infty} \frac{d\gamma}{2i\pi} \sqrt{\frac{1}{4\pi\Delta''(\frac{1-\gamma}{2}) y}}$$

---

<sup>12</sup>The mean squared transverse momentum  $\langle P_T^2 \rangle$  is presently known [24] only on a global average to be of order  $7GeV^2$ . It could depend on other variables but it happens to be very similar to the diffractive photoproduction slope, confirming the stability of this non-perturbative parameter in different kinematical regions. We shall assume it constant in the following.

$$\Theta Pf_{T,L} \exp \left\{ 2y[\Delta \left( \frac{1-\gamma}{2} \right)] + (Y-y) [\Delta(\gamma)] + 2\gamma \log \frac{Q}{Q_0} \right\} . \quad (11)$$

For comparison the QCD dipole formula for the total proton structure functions [13] is:

$$F_{T,L} = \mathcal{N}^{tot} \int_{c-i\infty}^{c+i\infty} \frac{d\gamma}{2i\pi} e^{Y\Delta(\gamma)} \left( \frac{Q}{Q_0} \right)^{2\gamma} h(\gamma) I_{T,L}(\gamma), \quad (12)$$

with

$$\mathcal{N}^{tot} = \frac{\alpha_s^2 N_c}{\pi} n_{eff} e_f^2 . \quad (13)$$

In order to proceed further in our theoretical analysis, it is suitable to look for an analytical solution of (11). For this sake we shall now use another saddle-point approximation near  $\gamma = 0$ . In previous analyses, the integral was either approximated in some regions of the variables [12] or numerically evaluated [23]. For sake of a theoretical discussion in parallel with the formula (12) for the total structure functions, we better choose a gaussian approximation valid in a reasonably large physical region.

The gaussian approximation makes use of the following expansions

$$\begin{aligned} \Delta \left( \frac{1-\gamma}{2} \right) &\approx \Delta + \frac{\Delta''}{8} \gamma^2 + \mathcal{O}(\gamma^4) \\ \Delta(\gamma) &\approx \Delta + \frac{\Delta''}{2} \left( \frac{1}{2} - \gamma \right)^2 + \mathcal{O} \left( \left( \frac{1}{2} - \gamma \right)^4 \right) , \end{aligned} \quad (14)$$

where by definition

$$\Delta \equiv \Delta(\gamma = \frac{1}{2}) = 4 \log 2 \frac{\alpha_s N_c}{\pi}; \Delta'' \equiv \Delta''(\gamma = \frac{1}{2}) = 28\zeta(3) \frac{\alpha_s N_c}{\pi} . \quad (15)$$

Note that  $0 < \gamma < 1/2$ , which allows one to use the gaussian saddle-point for diffraction in a region avoiding the edges of integration<sup>13</sup>  $\gamma = 0, \frac{1}{2}$ .

It is important to realize here a different expected result with the gaussian approximation for the total structure function (12) in the BFKL formalism

---

<sup>13</sup>We checked the approximate validity of the gaussian approximation by comparison with a non-Gaussian one  $\Delta(\gamma) \approx \frac{\alpha_s N_c}{\pi} \left( \frac{1}{\gamma} + 4\zeta(3) \gamma^2 \right)$  valid when  $\gamma \sim 0$  [12] and with numerical estimates [23]. More precisely,  $4 \log 2 \approx 2.77$ ;  $28\zeta(3) \approx 33.6$ , giving  $\Delta''/8\Delta$  of order 1. Hence the approximations (14) will be good for  $\Delta(\frac{1-\gamma}{2})$ , less for  $\Delta(\gamma)$ , but enough for our theoretical purpose.

where one uses a saddle-point approximation near  $\gamma = 1/2$ . In particular, the dynamical exponent  $\Delta(\gamma)$  will be moved away from its canonical value at  $\gamma = 1/2$ , even without the virtuality factor  $\left(\frac{Q}{Q_0}\right)^{2\gamma}$ .

After using the gaussian approximation, and relation (10), the resulting structure functions read:

$$F_{T,L}^{Diff}(Q^2, Y, y) = \mathcal{N}^{Diff} \frac{\langle P_T^2 \rangle}{x_P Q_0^2} \Theta(Pf_{T,L}) \frac{\exp(2y\Delta)}{4\pi\Delta''y} \times \sqrt{\frac{2}{1+2\eta}} \exp\{(Y-y)\epsilon_s\} \left(\frac{Q}{Q_0}\right)^{2\gamma_s} \exp\left(-\frac{2\eta}{1+2\eta} \frac{2\log^2\left(\frac{Q}{Q_0}\right)}{\Delta''(Y-y)}\right), \quad (16)$$

where the saddle-point determines both the new “effective dimension” and “effective intercept”:

$$\gamma_s = \frac{\eta}{1+2\eta}; \quad \epsilon_s = \Delta + \frac{\Delta''}{8(1+2\eta)} \quad (17)$$

for the Pomeron-photon cross-section. By definition

$$\eta = \frac{Y-y}{y} = \frac{\log 1/\beta}{\log 1/x_P}. \quad (18)$$

The connection between the QCD dipole model and the partonic Pomeron is thus well illustrated by the identification of our resulting formula (16) with the triple Regge prediction (2) considered at  $t = 0$ . Indeed, We identify the partonic Pomeron intercept as  $\alpha_P(0) \equiv 1 + \Delta$ , which is natural in a BFKL framework at  $Q = Q_0$ , see the following discussion. We get now the following new relation:

$$\sigma_{\gamma^* - P}^{tot} \sim \sqrt{\frac{2}{1+2\eta}} \exp\{(Y-y)\epsilon_s\} \left(\frac{Q}{Q_0}\right)^{2\gamma_s} \exp\left(-\frac{2\eta}{1+2\eta} \frac{2\log^2\left(\frac{Q}{Q_0}\right)}{\Delta''(Y-y)}\right), \quad (19)$$

with (17) defining the “effective” anomalous dimension and intercept of a “deformed” BFKL formula for the photon Pomeron (with zero mass  $= \sqrt{-t}$ ) total cross-section.

It is interesting to compare expression (16) and  $\gamma_s, \epsilon_s$  with the canonical BFKL formula (12) in the saddle-point approximation namely:

$$F_{L,T} \approx \mathcal{N}^{tot} h I_{T,L} \frac{\exp(Y\Delta)}{\sqrt{2\pi\Delta'' Y}} \left(\frac{Q}{Q_0}\right) \exp\left(-\frac{2\log^2\left(\frac{Q}{Q_0}\right)}{\Delta'' Y}\right). \quad (20)$$

The “effective BFKL” parameters for  $\sigma_{\gamma^* P}^{tot}$  differ from the BFKL ones by an amount depending on  $\eta = \frac{Y-y}{y}$ . Also note that the “diffusion” term, which quantifies the amount of transverse momentum drift of gluons (or dipoles) along the BFKL evolution [25] is renormalized by a factor  $2\eta/(1+2\eta)$ , the same as for the anomalous dimension  $\gamma_s$ .

While at large  $\eta$  the formulae become similar, since for instance  $\gamma_s \rightarrow \frac{1}{2}, \epsilon_s \rightarrow \Delta$ , they sizeably differ from them provided  $\eta \geq \mathcal{O}(1)$ . In fact, this is realized in practice, since in present experiments  $\beta \geq x_P$ . On contrary, the features of the Pomeron exchanges responsible for the gaps are those of the “bare” BFKL values taken at  $Q \equiv Q_0$ , which can be interpreted as the partonic Pomerons in the BFKL formalism since the scale  $Q_0$  is characteristic of the starting point of the QCD evolutions.

Thus the “deformed” BFKL parameters (17) lead to a situation which can be called intermediate between a “hard” (with effective dimension  $\gamma = \frac{1}{2}$ ) and a “soft” (with  $\gamma = 0$ ) Pomeron, depending on the ratio  $2\eta/(1+2\eta)$ . Also, the energy dependence is faster for the “deformed” BFKL singularity than for the partonic Pomeron. This original situation is confirmed by numerical estimates [23].

## 4 From dipoles to Soft Colour Interaction

In order to confront and unify the QCD dipole and Soft Colour Interaction approaches, we will estimate the overall contribution of hard diffraction to the total structure function at fixed value of  $x_{Bj}$ . As previously done, we will stick here to the “inelastic” (leading-twist) diffractive component leaving for further study the “elastic” component with small diffractive masses.

Let us then consider the following integral:

$$\begin{aligned}
F_{T,L}^{Diff/tot} &= \int_{x_{Bj}}^{x_{gap}} dx_P dP_T^2 \frac{dF_{T,L}^{Diff}}{dP_T^2}(Q^2, Y, y; P_T) \\
&\approx \int_{x_{Bj}}^{x_{gap}} dx_P dP_T^2 \langle P_T^2 \rangle \frac{dF_{T,L}^{Diff}}{dP_T^2}(Q^2, Y, y; P_T = 0) \\
&= \frac{\mathcal{N}^{Diff} \langle P_T^2 \rangle}{Q_0^2} \int_{c-i\infty}^{c+i\infty} \frac{d\gamma_1}{2i\pi} \frac{d\gamma_2}{2i\pi} \frac{d\gamma}{2i\pi} \delta(1-\gamma_1-\gamma_2-\gamma) \Theta P f_{T,L} \\
&\times \left( \frac{Q}{Q_0} \right)^{2\gamma} \int_{y_{gap}}^Y dy e^{[y(\Delta(\gamma_1) + \Delta(\gamma_2)) + (Y-y)\Delta(\gamma)]}, \tag{21}
\end{aligned}$$

where  $y_{gap} \equiv \log \frac{1}{x_{gap}}$  is the minimal value retained for the rapidity gap. Indeed, the integral over  $y$  is expected to be dominated by the behaviour of the integrand for large enough gaps. We also keep the approximation<sup>14</sup>  $\langle P_T^2 \rangle = cst$ .

Technically, the integrals in (21) can be performed using a saddle-point method in both variables  $\gamma$  and  $y$  provided the conditions

$$\Delta Y \gg 1 ; \frac{\log \frac{Q}{Q_0}}{\Delta'' Y} \leq 1 \quad (22)$$

are realized. The saddle-point equations, see Appendix **A2**, lead to remarkably simple solutions

$$\begin{aligned} y_c &= \left( Y + \frac{2 \log \frac{Q}{Q_0}}{\Delta'(\gamma_c)} \right) \left( 1 + \frac{\Delta' \left( \frac{1-\gamma_c}{2} \right)}{\Delta'(\gamma_c)} \right)^{-1} \\ \Delta(\gamma_c) &= 2\Delta \left( \frac{1-\gamma_c}{2} \right) \end{aligned} \quad (23)$$

resulting in a value of  $\gamma_c \simeq 0.175$  which is “universal”, i.e. independent of the kinematics of the reaction.

The saddle-point calculation leads to the following expression:

$$F_{T,L}^{Diff/tot} = \mathcal{N}^{Diff} \frac{\langle P_T^2 \rangle}{Q_0^2} \frac{\Theta P f_{T,L}}{|\Delta' \left( \frac{1-\gamma_c}{2} \right) - \Delta'(\gamma_c)|} \left( \frac{Q}{Q_0} \right)^{2\gamma_c} \frac{\exp(Y\Delta(\gamma_c))}{\sqrt{4\pi\Delta'' \left( \frac{1-\gamma_c}{2} \right) y_c}}. \quad (24)$$

Note that  $\Delta' \left( \frac{1-\gamma_c}{2} \right) + \Delta'(\gamma_c) < 0$  when  $0 < \gamma < \frac{1}{2}$ .

Let us now come to the main outcome of this calculation. Let us compare the result (24) to a *total* hard contribution of BFKL type, see equation (12), which can be rewritten in a saddle-point approximation:

$$F_{L,T} \approx \mathcal{N}^{tot} h(\gamma_{s.p.}) I_{T,L}(\gamma_{s.p.}) \left( \frac{Q}{Q_0} \right)^{2\gamma_{s.p.}} \frac{\exp(Y\Delta(\gamma_{s.p.}))}{\sqrt{2\pi\Delta'' Y}}, \quad (25)$$

with the BFKL saddle-point value

$$\gamma_{s.p.} = \frac{1}{2} \left( 1 - 4 \frac{\log \left( \frac{Q}{Q_0} \right)}{\Delta'' Y} \right). \quad (26)$$

---

<sup>14</sup>See the discussion at the end of section 2 and footnote 12.

Hence, (24) is strikingly similar to a BFKL formula (12) with a shift in the value of the saddle-point namely:

$$\gamma_{s.p.} \Rightarrow \gamma_c . \quad (27)$$

It is remarkable that the total diffractive contribution to the structure function has the same analytical form as the non-diffractive one, up to the substitution (27) and the prefactors, which we will study next. This QCD derivation is thus compatible with the postulate of the Soft Colour Interaction approach, namely the relation between the diffractive and non diffractive deep-inelastic processes stating that the diffractive part of the total hard cross-section is not intrinsically different. In the SCI framework, this is explicitly realized as a whole in the first paper of Ref. [8] while it is realized graph by graph in the approach of paper [9]. In the framework of our QCD calculations, it is however realized in a somewhat modified way, through a shift (27) in the “effective” parameters of the hard interaction. We will comment later upon possible phenomenological consequences of this effect.

Using our identification of the hard interaction of BFKL type present in  $F_{T,L}^{Diff/tot}$ , we are now able to take advantage of the second postulate of the Soft Colour Interaction approach, i.e. the probabilistic evaluation of the soft rearrangement of colour at large distances, leading to the famous factor  $1/N_c^2$  in the ratio of diffractive vs. non diffractive cross-sections. This beautifully simple proposal expected from non perturbative QCD properties can be incorporated in the unified approach in an easy way. We are thus led to a proportionality between the prefactors of the BFKL expressions (20) and (24), namely

$$\frac{\mathcal{N}^{Diff} \langle P_T^2 \rangle}{Q_0^2} \frac{\Theta P f_{T,L}(\gamma)}{|\Delta'(\frac{1-\gamma}{2}) + \Delta'(\gamma)|} \iff \frac{1}{N_c^2} \mathcal{N}^{tot} h(\gamma) I_{T,L}(\gamma) . \quad (28)$$

Using our result (24) and assuming thus a relation between the prefactors compatible with (28), the total diffractive contribution can be rewritten

$$F_{T,L}^{Diff/tot} \approx \frac{1}{N_c^2} \mathcal{N}^{tot} h(\gamma_c) I_{T,L}(\gamma_c) \left( \frac{Q}{Q_0} \right)^{2\gamma_c} \frac{\exp(Y\Delta(\gamma_c))}{\sqrt{4\pi\Delta''(\frac{1-\gamma_c}{2})y_c}} . \quad (29)$$

Coming back now to our saddle-point result (16) for the differential hard diffractive structure function (5), one rewrites

$$F_{T,L}^{Diff}(Q^2, Y, y) \approx \frac{1}{N_c^2} \frac{\mathcal{N}}{x_P} \frac{e^{2y\Delta}}{4\pi\Delta''y} \sqrt{\frac{2}{1+2\eta}}$$

$$\times \exp \{(Y-y) \epsilon_s\} \left( \frac{Q}{Q_0} \right)^{2\gamma_s} \exp \left( -\frac{2\eta}{1+2\eta} \frac{2 \log^2 \left( \frac{Q}{Q_0} \right)}{\Delta''(Y-y)} \right), \quad (30)$$

where  $\gamma_s$  and  $\epsilon_s$  are defined in (17) and a *known* normalization

$$\mathcal{N} \equiv \left| \Delta' \left( \frac{1-\gamma_c}{2} \right) + \Delta'(\gamma_c) \right| h(\gamma_c) I_{T,L}(\gamma_c) \times \mathcal{N}^{tot}, \quad (31)$$

with  $\gamma_c$  as in (29). Note that we could also have considered  $\gamma_s(y)$  instead of the constant  $\gamma_c$  in formula (31) since the prefactors are expected to be slowly varying functions of  $\gamma$ . In fact, care must be taken about poles at  $\gamma = 0$  contained in the functions  $I_{T,L}(\gamma)$  (the same poles appear consistently in both sides of (28), as explicit in the definition (8) of  $Pf_{T,L}(\gamma)$ ). A normalization correction could appear in (29,30) by a known rescaling factor [26]. We leave a detailed phenomenological study for further work.

The relations (29,30) call for some comments. On a theoretical point of view, these relations are out of range of the present knowledge of QCD, for its large distance, confining regime. However, some arguments are in favor of such kind of relations. For instance, there exists a complementarity between the perturbative results and the non perturbative ansatze present here. The value of the strong coupling constant  $\alpha_s$ , the number of primordial dipoles  $n_{eff}$  and, in the derivation [23] of hard diffraction, the expression of the cut-off  $\Theta$  are not determined in the BFKL approach which essentially means that the relative normalization of diffractive vs. non-diffractive contributions remain unknown. It is just this ratio which is determined by the Soft Colour Interaction ansatz. On the other hand, the non-trivial form of the structure functions inherited from the QCD dipole calculations could not be guessed just from what we know about soft colour processes, which are limited by our present lack of knowledge of the theory of strong interactions at long distances.

## 5 Summary and outlook

Summarizing our results, let us quote:

- 1) Using S-Matrix properties of triple-Regge contributions, a relation is found between three popular approaches to hard diffraction: the partonic Pomeron, Soft Colour Interaction and QCD dipole formulations.

**2)** A formulation of the Soft Colour Interaction approach is proposed as a specific double discontinuity of a  $3 \rightarrow 3$  forward amplitude.

**3)** The “effective” parameters of the  $\gamma_c$ -Pomeron total cross-section corresponding to the partonic Pomeron are determined from leading log perturbative QCD resummation. They are found to depend not only on  $Q^2$  but also on rapidities through the parameter  $\eta = \log(1/\beta)/\log(1/x_P) \approx <\log(M_X^2)>/y_{gap}$ .

**4)** The diffractive structure functions  $F_{T,L}^{Diff}(Q^2, Y, y)$  are found to be determined both in form and normalization, using their perturbative (through QCD dipoles) and non perturbative (through Soft Color Interaction) relationship with the total structure functions  $F_{T,L}^{tot}(Q^2, Y, y)$ .

Let us add a few comments concerning these points.

Concerning the *partonic Pomeron* approach, we find<sup>15</sup> that the “effective” parameters of  $\sigma_{\gamma^* - P}^{(T,L)/tot}$  depend on a parameter  $\eta$  external to the  $\gamma^* - P$  reaction. Looking to the deep reason of this fact, we find the constraint  $\gamma_1 + \gamma_2 + \gamma = 1$  which prevents the BFKL Pomeron singularities of the involved BFKL Pomerons from taking their ordinary saddle-point positions. Hence those Pomerons responsible for the gaps become  $Q^2$ -independent while the one in  $\sigma_{\gamma^* - P}^{(T,L)/tot}$  becomes both  $Q^2$  and  $\eta$ -dependent. This kind of “off-shellness” is quite remarkable, showing that a universal Pomeron kernel  $\Delta(\gamma)$  can lead to non-universal effective behaviours when put in a hard interaction context. It would be interesting to look for an experimental study of this intriguing feature of the partonic Pomeron. The compatibility with DGLAP evolution equations is also to be studied in detail.

Concerning the *Soft Colour Interaction* prediction, relating the diffractive and non-diffractive components of deep-inelastic scattering, it seems quite compatible with the QCD predictions on the form of the amplitudes. However, an unexpected difference appears, since the typical values of the “effective” dimensions are different in both cases. It is clear for the integrated diffractive contribution  $F_{T,L}^{Diff/tot}$ , see (21), comparing  $\gamma_{s.p.}$  and  $\gamma_c$ . It is also explicit from the analysis of  $F_{T,L}^{Diff}$  itself that the relevant regions in the inverse Mellin transforms are always for values of  $\gamma$  lower than for  $F_{T,L}^{tot}$ . It will be interesting to test this prediction with data.

For developing this study beyond the first theoretical step, we would like to stress the feasibility of phenomenological tests and applications. How-

---

<sup>15</sup>This remark was made in Ref.[12] about the BFKL result and is extended here to the partonic Pomeron.

ever this requires a similar analysis for the “elastic” QCD dipole component. One knows that the Mueller Regge formulae can be extended to generalized Pomeron Regge amplitudes (e.g. [27]). We find interesting to elaborate on the S-matrix discontinuity properties in this context and their possible relations with “higher-twist” QCD contributions which are known to be relevant in this case. This deserves a specific study which is beyond the scope of this paper.

On the theoretical ground, some interesting problems arise. For instance, the known problem of the application of a (resummed) perturbative scheme at  $t \neq 0$  require a better understanding of the matching between perturbative and non-perturbative features. Also are interesting to develop the more precise extension of this scheme to Regge cuts, next-leading BFKL contributions and, last but not least, unitarity corrections, which are required to identify properly the soft Pomeron contributions. Finally, the study of Tevatron results on diffraction will be welcome, since the Soft Colour Interaction approach seems to give some interesting clues, while factorization of the parton structure functions of the Pomeron appears to be violated.

### **Acknowledgements**

Thanks are due to Jochen Bartels, who draw the attention of one of us (R.P.) to the relations between Regge discontinuities cf. the papers [12, 22], to Andrzej Bialas for fruitful discussions and the inspiring paper in collaboration with Wiesław Czyz [23], and to Christophe Royon, for his help and advice.

## APPENDIX: Saddle-point calculation of section 4

Starting with Eq. (21), the integration over  $\gamma_1 - \gamma_2$  leads to

$$F_{T,L}^{Diff} = \mathcal{N}^{Diff} \frac{P_T^2}{x_P Q_0^2} \int_{c-i\infty}^{c+i\infty} \frac{d\gamma}{2i\pi} \sqrt{\frac{1}{4\pi\Delta''(\frac{1-\gamma}{2}) y}} \Theta P f_{T,L} \exp \mathcal{H}(y, \gamma) , \quad (32)$$

where the function

$$\mathcal{H}(y, \gamma) \equiv \left\{ 2y\Delta\left(\frac{1-\gamma}{2}\right) + (Y-y)\Delta(\gamma) + 2\gamma \log \frac{Q}{Q_0} \right\} \quad (33)$$

determines the saddle-point equations, namely

$$\begin{aligned} \frac{\partial \mathcal{H}(y, \gamma)}{\partial \gamma} &\equiv -y\Delta'\left(\frac{1-\gamma}{2}\right) + (Y-y)\Delta'(\gamma) + 2\log \frac{Q}{Q_0} = 0 \\ \frac{\partial \mathcal{H}(y, \gamma)}{\partial y} &\equiv 2\Delta\left(\frac{1-\gamma}{2}\right) - \Delta(\gamma) = 0 , \end{aligned} \quad (34)$$

whose solution  $(y_c, \gamma_c)$  is given in (23), see the text.

The prefactors appearing in the integrated formula are coming from the partial second derivatives of  $\mathcal{H}(y, \gamma)$ . A first one comes from the partial second derivative over  $\gamma$

$$\frac{1}{\sqrt{2\pi \frac{\partial^2 \mathcal{H}}{\partial \gamma^2}(y_c, \gamma_c)}} = \frac{1}{\sqrt{2\pi \left[ \frac{y_c}{2}\Delta''\left(\frac{1-\gamma_c}{2}\right) + (Y-y_c)\Delta''(\gamma_c) \right]}} . \quad (35)$$

The second one is slightly more involved. It reads

$$\sqrt{\frac{2\pi}{\frac{\partial \gamma_c}{\partial y} \left[ 2\frac{\partial^2 \mathcal{H}}{\partial \gamma \partial y} + \frac{\partial^2 \mathcal{H}}{\partial \gamma^2} \frac{\partial \gamma_c}{\partial y} \right]}} = \sqrt{\frac{2\pi \left[ \frac{y_c}{2}\Delta''\left(\frac{1-\gamma_c}{2}\right) + (Y-y_c)\Delta''(\gamma_c) \right]}{\left( \Delta'\left(\frac{1-\gamma_c}{2}\right) + \Delta'(\gamma_c) \right)^2}} . \quad (36)$$

The simplification appearing in the second prefactor comes from an identity

$$\frac{\partial^2 \mathcal{H}}{\partial y^2} \frac{\partial \gamma_c}{\partial y} + \frac{\partial^2 \mathcal{H}}{\partial \gamma \partial y} = 0 \quad (37)$$

at the saddle-point  $(y_c, \gamma_c)$ , which came from the calculation.

Noting that the numerator of (36) simplifies with the denominator of (35), we are led to the final remarkably simple formula (24) of the text.

## References

- [1] C. Ahmed et al., H1 coll., *Phys. Lett.* **B348** (1995) 681; M. Derrick et al., ZEUS coll., *Z.Phys.* **C68** (1995) 569.
- [2] F. Abe et al., CDF coll., *Phys. Rev. Lett.* **78** (1997) 2698; **79** (1997) 2636; **80** (1998) 1156; S. Abachi et al., D0 coll., *Phys. Lett.* **B440** (1998) 5278. T. Affolder et al., CDF coll., *Phys. Rev. Lett.* **84** (2000) 5043; **85** (2000) 4215.
- [3] UA8 Coll., R. Bonino et al., *Phys. Lett.* **B211** (1988) 239.
- [4] G. Ingelman, P. Schlein, *Phys. Lett.* **B152** (1985) 256.
- [5] For an up-to-date analysis and previous references, see: C. Royon, L. Schoeffel, J. Bartels, H. Jung, R. Peschanski, [hep-ph/0010015] *Phys. Rev.* **D63** (2001) 074004.
- [6] A. Kaidalov, *Phys. Rept.* **50** (1979) 157.
- [7] A. Capella, A. Kaidalov, C. Merino, J. Tran Thanh Van, [hep-ph/9408212], *Phys. Lett.* **B343** (1995) 403; A. Capella, A. Kaidalov, C. Merino, D. Perermann, J. Tran Thanh Van [hep-ph/9506454], *Phys. Rev.* **D53** (1996) **2309** (1996) 2309.
- [8] W. Buchmuller, A. Hebecker, [hep-ph/9504374], *Phys. Lett.* **B355** (1995) 573; [hep-ph/9512329], *Nucl. Phys.* **B476** (1996) 203. An extensive review of this and other approaches can be found in A. Hebecker, [hep-ph/9905226], *Phys. Rep.* **331** (2000) 1.
- [9] A. Edin, G. Ingelman, J. Rathsman, [hep-ph/9605281], *Z. Phys.* **C75** (1997) 57. For a review and discussion including tevatron results, see: G. Ingelman, [hep-ph/9912534], Lectures at St. Croix summer school 1998: *Techniques and Concepts of High Energy Physics X*, Ed. T. Ferbel, Kluwer Academic Publishers 1999, p. 597.
- [10] L.N. Lipatov, *Sov. J. Nucl. Phys.* **23** (1976) 642; V.S. Fadin, E.A. Kuraev and L.N. Lipatov, *Phys. Lett.* **B60** (1975) 50; E.A. Kuraev, L.N. Lipatov and V.S. Fadin, *Sov. Phys. JETP* **44** (1976) 45, **45** (1977) 199; I.I. Balitsky and L.N. Lipatov, *Sov. J. Nucl. Phys.* **28** (1978) 822; L.N. Lipatov *Zh. Eksp. Teor. Fiz.* **90** (1986) 1536 (Eng. trans. *Sov. Phys. JETP* **63** (1986) 904).

- [11] A. H. Mueller, B. Patel, *Nucl. Phys.* **B425** (1994) 471;  
 A.Bialas, H.Navelet, R.Peschanski, *Phys. Lett.* **B427** (1998) 147.  
 For a related approach, mixing perturbative and non-perturbative considerations, see: N. N. Nikolaev, B. G. Zakharov, *Z. Phys.* **C49** (1991) 607; *Z. Phys.* **C53** (1992) 331.
- [12] J. Bartels, M. Wusthoff, *Zeit. fur Phys.* **C66** (1995) 157.
- [13] H.Navelet, R.Peschanski and C.Royon, *Phys. Lett.* **B366** (1996) 329; H. Navelet, R. Peschanski, Ch. Royon, S. Wallon, *Phys. Lett.* **B385** (1996) 357.
- [14] A. Bialas, R. Peschanski, *Phys. Lett.* **B378** (1996) 302; **B387** (1996) 405.  
 A.Bialas, R.Peschanski and C.Royon, *Phys. Rev.* **D57** (1998) 6899; S.Munier, R.Peschanski and C.Royon, *Nucl. Phys.* **B354** (1998) 297.
- [15] M.Genovese, N.N. Nikolaev, B.G. Zakharov, *J. Exp. Theor. Phys.* **81** (1995) 625.
- [16] M. Genovese, N. N. Nikolaev, B. G. Zakharov, *J. Exp. Theor. Phys.* **81** (1995) 625, 633.
- [17] A. Mueller, *Phys. Rev.* **D2** (1970) 2963, **D4** (1971) 150.
- [18] C.E. DeTar, C.E. Jones, F.E. Low, J.H. Weis, J.E. Young, C-I Tan, *Phys. Rev. Lett.* **26** (1971) 675. For a detailed account of the origin of the Soft Pomeron formula, see W.R. Frazer, *Rev. Mod. Phys.* **44** (1972) 284.
- [19] C.E. DeTar, K. Kang, C-I Tan, J.H. Weis, *Phys. Rev.* **D4** (1971) 425. For a review and references, see R.C. Brower, C.E. DeTar, J.H. Weis, *Phys. Rept.* **14** (1974) 257.
- [20] S. Catani, M. Ciafaloni, F. Hautmann, *Nucl. Phys.* **B366** (1991) 135. J. C. Collins, R. K. Ellis, *Nucl. Phys.* **B360** (1991) 3. E. M. Levin, M. G. Ryskin, Yu. M. Shabelskii, A. G. Shuvaev, *Sov. J. Nucl. Phys.* **53** (1991) 657.
- [21] J. Bartels, J. Ellis, H. Kowalski, M. Wuesthoff, *Eur. Phys. J.* **C7** (1999) 443; J. Bartels, C. Royon, *Mod. Phys. Lett.* **A14** (1999) 1583.

- [22] J. Bartels, H. Lotter, M. Wusthoff, *Zeit. fur Phys.* **C68** (1995) 121.
- [23] A.Bialas, W.Czyz, hep-ph/9808437, *Acta Phys. Polon.* **B29** (1998) 2095.
- [24] ZEUS Collaboration; J.Breitweg et al. *Eur. Phys. Jour.* **C1** (1998) 81;  
For the diffractive photoproduction slope, see :*Eur. Phys. Jour.* **C2** (1998) 2.
- [25] J. Bartels, *J. Phys.* **G19** (1993) 1611.
- [26] Ch. Royon, private communication.
- [27] See, for instance the review papers by Ph. Salin, *Gif-sur-Yvette summer school*, September 24 -October 6 (1973), in French; D. Horn, *Phys. Rep.* **4** (1972) 1.